Available online at www.sciencedirect.com
ScienceDirect
Journal of Catalysis 247 (2007) 368–378
JOURNAL OF CATALYSIS
www.elsevier.com/locate/jcat

Aromatization of methanol and methylation of benzene over Mo_2C/ZSM-5 catalysts

Róbert Barthos, Tamás Bánsági, Tímea Süli Zakar, Frigyes Solymosi *

Institute of Solid State and Radiochemistry, University of Szeged and Reaction Kinetics Research Group of the Hungarian Academy of Sciences, P.O. Box 168, H-6701 Szeged, Hungary

Received 30 October 2006; revised 19 February 2007; accepted 21 February 2007

Abstract

The adsorption and reaction pathways of methanol were investigated on various Mo_2C-containing catalysts characterized by XPS and surface acidity measurements. FTIR spectroscopy indicated the formation of a strongly bonded methoxy species on Mo_2C/ZSM-5(80) at 300 K that which was converted into adsorbed dimethyl ether at 373–473 K. TPD experiments following the adsorption of methanol on both ZSM-5 and Mo_2C/ZSM-5 at 300 K showed desorption profiles corresponding to unreacted methanol and decomposition products (H_2, CH_2O, CH_3CHO, CH_3–O–CH_3, and C_2H_4). Unsupported Mo_2C catalyzes only the decomposition of methanol. The same feature was observed for silica-supported Mo_2C. But a completely different picture was obtained when ZSM-5 was used as a support, which is known to be an active material in converting methanol into ethylene. The aromatization of methanol also occurred on this zeolite, but to only a limited extent. The deposition of Mo_2C on ZSM-5 markedly enhanced the formation of aromatics (benzene, toluene, xylene and C_{9+}), however. The highest yield of the formation of aromatics was measured for 5% Mo_2C/ZSM-5 ($SiO_2/Al_2O_3 = 80$) at 773 K. It is assumed that Mo_2C opens a new route for the activation of methanol and also for the reactions of ethylene thus formed. Further experiments showed that Mo_2C/ZSM-5(80) was able to catalyze the methylation of benzene with methanol, which explains the formation of toluene, xylenes, and C_{9+} aromatics in the reaction of methanol alone.

Keywords: Aromatization of methanol; Decomposition of methanol; Methylation of benzene Mo_2C; Mo_2C/ZSM-5; Mo_2C/SiO_2

1. Introduction

The direct conversion of alkanes into aromatics is an important process for industry, and thus extensive research on this reaction has been performed. The results obtained on various catalysts and the possible mechanism of this complex process are well documented in several excellent reviews [1–6]. Previous studies have demonstrated that depending on the reaction conditions and on the catalyst systems, methanol also can be transferred into olefins and aromatics on ZSM-5 zeolites [7–16]. The latter process is promoted by Ga and, more particularly, by Zn additive [12–16]. Recently it has been found that Mo_2C is also an effective promoter in the aromatization of several hydrocarbons and ethanol occurring on ZSM-5 [17–25]. Moreover, this catalyst exhibits a unique behavior in that it can convert methane into benzene with 80% selectivity at 10–15% conversion, which ZSM-5 alone or promoted with Zn and Ga cannot do [26–32]. Based on this finding, it seemed worthwhile to examine the influence of Mo_2C on the reaction and aromatization of CH_3OH on ZSM-5 and other oxidic supports.

2. Experimental

2.1. Methods

Catalytic reaction was carried out at 1 atm of pressure in a fixed-bed, continuous-flow reactor comprising a quartz tube connected to a capillary tube [23,24]. The flow rate was 40 mL/min, the carrier gas was Ar, and the methanol content of the carrier gas was 10%. A ~0.3 g catalyst sample was loosely compressed and broken into small (1–2 mm) fragments. Reaction products were analyzed by gas chromatography using a Hewlett-Packard 6890 gas chromatograph equipped with a

---

* Corresponding author. Fax: +36 62 420 678.
E-mail address: fsolym@chem.u-szeged.hu (F. Solymosi).

0021-9517/$ – see front matter © 2007 Elsevier Inc. All rights reserved.
doi:10.1016/j.jcat.2007.02.017

thermal conductivity detector for the analysis of H_2, CO, CO_2, H_2O; a flame ionization detector for the analysis of organic compounds; and PORAPAK Q + PORAPAQ S columns. The calibration of all compounds was carried out separately. We note that the values determined for individual compounds were not altered by the presence of any other major products. The conversion of methanol was calculated taking into account the amount consumed. The selectivity for reaction products, S, was defined as

$$S_i = \frac{x_i n_i}{\sum_i x_i n_i},$$

where x_i is the fraction of product i, and n_i is the number of carbon atoms in each molecule of gaseous products. FTIR spectra of adsorbed gases were recorded with a Biorad (Digilab. Div. FTS 155) instrument with a wave number accuracy of $\pm 4\ \text{cm}^{-1}$. All the spectra presented are difference spectra. The background was the spectrum of the pretreated sample before the adsorption of reactants. Temperature-programmed desorption (TPD) curves were obtained by quadrupole mass spectrometry.

The adsorption of methanol (10% in helium carrier gas) was flown through the catalyst for 15 min at 300–304 K. The catalyst was then purged with pure He to remove any weakly adsorbed methanol and lined for 90 min. The gas flow was introduced to the UHV system via a quartz capillary tube containing a leak UHV valve. A constant operating pressure of 8×10^{-6} Torr was maintained in the system during all TPD runs. TPD experiments were performed using a He flow of 40 mL/min and a heating rate of 10 K/min from 300 to 873 K.

The acidic properties of catalysts have been determined by NH_3-TPD and FTIR methods using the adsorption of pyridine and CO, as described previously [24]. The XPS measurements were performed in a Kratos XSAM 800 instrument at a base pressure of 10^{-8} Torr using Mg$K\alpha$ primary radiation (14 kV, 10 mA). To compensate for possible charging effects, binding energies (BEs) were normalized to the Fermi level for the Mo_2C. The amount of coke deposited on the catalyst during the reaction was determined by temperature-programmed reaction (TPR). The catalyst was cooled in flowing argon and then heated in a H_2 stream with a rate of 5 K/min; the hydrocarbons thus formed were then measured.

2.2. Materials

Mo_2C-containing catalysts were the same as used our other studies [23,24]. Unsupported Mo_2C was prepared by the carburization of MoO_3 (product of ALFA AESAR) by C_2H_6/H_2 [33]. The oxide was heated under a 10% v/v C_2H_6/H_2 gas mixture from room temperature to 900 K at a heating rate of 0.8 K/min. Afterward the sample was cooled to room temperature under argon. The carbide was passivated in flowing 1% O_2/He at 300 K. The surface area of Mo_2C is 20 m^2/g. In certain cases, Mo_2C was prepared in situ in the catalytic reactor when the last step was missing. Supported Mo_2C catalysts were prepared in a similar manner by the carburization of MoO_3-containing supports with C_2H_6/H_2 gas mixture. To remove the excess carbon deposited on the Mo_2C during preparation and the Mo–O species produced during passivation, the Mo_2C-containing catalyst was reduced before the catalytic measurements in situ in a H_2 stream for 60 min at 873 K. The MoO_3/support samples were prepared by impregnating the support with a basic solution of ammonium heptamolybdate to yield 2, 5, and 10 wt% of MoO_3. The suspension was dried and calcined at 863 K for 5 h. The following materials were used as supports: ZSM-5 with SiO_2/Al_2O_3 ratios of 30, 80, and 280 and BET areas of 400, 425, and 400 m^2/g, and SiO_2 (Aerosil, 380 m^2/g). CH_3OH was a product of SHARLAU with a purity of 99.9%.

3. Results

3.1. Characterization of the catalyst

All of the catalysts used in this study have been previously characterized by XPS measurements [23,24]. The BEs for Mo($3d_{5/2}$) and Mo($3d_{3/2}$) showed some slight variation with different samples, but dropped to 227.8–228.2 and 230.7–231.1 eV, respectively; that for C(1s) dropped to 283.8 eV. These values are consistent with those attributed to Mo_2C [34–36]. In terms of the acidity of the catalysts, we refer to our previous work, which used the same samples [24]. We found that during the preparation of Mo/ZSM-5 catalyst, Mo compounds reacted with OH groups of ZSM-5. As a result, the Brönsted sites decreased markedly in number, but were not completely eliminated. The greater the carbide content, the greater the decrease. At the same time, the Lewis acidity was somewhat enhanced by Mo_2C deposition.

3.2. FTIR and TPD measurements

The primary aim of the IR study was to determine the effect of Mo_2C on the adsorption of methanol on ZSM-5 and it surface processes. Fig. 1A shows the IR spectra of ZSM-5(80) after the adsorption of methanol at 300 K for 15 min, and subsequent heating of the sample to higher temperatures under continuous evacuation. Table 1 presents the absorption bands observed at 300 K, along contains the characteristic IR features of various compounds detected after the surface reaction of adsorbed methanol [37–47]. The heat treatment of adsorbed layer caused a gradual attenuation of absorption bands without any significant shift or appearance of new spectral features. We found the same features in the presence of 2 or 10% Mo_2C (Fig. 1B); however, after annealing the adsorbed layer, weak absorption features appeared at 2971 and 2925 cm^{-1}.

TPD spectra for various products are presented in Fig. 2. In the case of pure ZSM-5(80), the following compounds were formed: methanol ($T_p = 352$ K), methane ($T_p = 354$ K), formaldehyde ($T_p = 354$ and 470 K), H_2O ($T_p = 370$ and 542 K), C_2H_4 ($T_p = 531$ K), and H_2 ($T_p = 358$ K) (Fig. 2A). A small amount of dimethyl ether ($T_p \sim 520$ K) was also detected in the desorbing products. Calculation showed that the chemicals desorbed in the same peaks as methanol are mostly its fragments. When 2% Mo_2C was deposited on ZSM-5(80), only slight variations were experienced in the peak temperatures and in the amounts of desorbed compounds. At 10% Mo_2C content, however, new high-temperature peaks developed for H_2 ($T_p = 574$ K), CO ($T_p = 591$ K), and CH_4 ($T_p = 572$ K) (Fig. 2B). The characteristics of the desorption of other products remained practically unaltered.

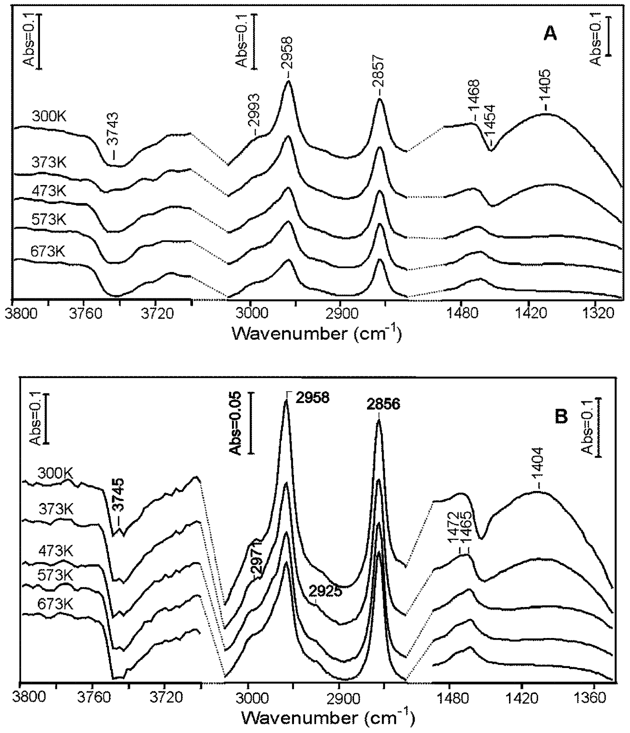

Fig. 1. FTIR spectra of ZSM-5(80) (A) and 2% Mo_2C/ZSM-5(B) following the adsorption of methanol (1.5 Torr) at 300 K, and after heating the samples to different temperatures during continuous degassing.

3.3. Reaction of methanol

3.3.1. Pure Mo_2C catalyst

Mo_2C prepared by a C_2H_6/H_2 gas mixture exhibited high activity. The decomposition of methanol was observed at very low temperature (473 K). At 623 K, the conversion already reached ~90%. Besides hydrogen, CO, CO_2, and methane were the main carbon-containing products. Aromatic compounds were detected only in trace amounts even at 773 K. The formation of dimethyl ether also occurred; however, its selectivity remained below ~6% in the temperature range of 573–773 K.

3.3.2. Supported Mo_2C catalyst

By depositing 2 or 10% Mo_2C in highly dispersed state on silica, we obtained a somewhat more effective catalyst. The main C-containing products at 573 K were methane ($S = 35\%$), CO ($S = 11\%$), and dimethyl ether ($S = 32\%$). Whereas the selectivity of the first two compounds increased with increasing temperature, that of dimethyl ether decreased and almost disappeared at 773–873 K. Interestingly, ethylene was formed with low selectivity, a maximum with 2.5% at 573–873 K. There was no sign of formation of any aromatics.

Better results were obtained using zeolites. In harmony with the previous studies [4,7–16], the ZSM-5 alone was an active material in converting methanol into other compounds. The reaction on ZSM-5 samples was observed at very low temperatures (423–473 K), yielding mostly dimethyl ether. The conversion reached 99% even at 573 K. At this temperature, the formation of several olefins and aromatics (benzene, toluene, xylenes, and C_{9+}) was seen. The production of aromatics depended on the Si/Al ratio; it was the highest on ZSM-5(30) and the lowest on ZSM-5(280) (Table 2). A general feature of ZSM-5 samples is that the selectivity of ethylene and propylene grad-

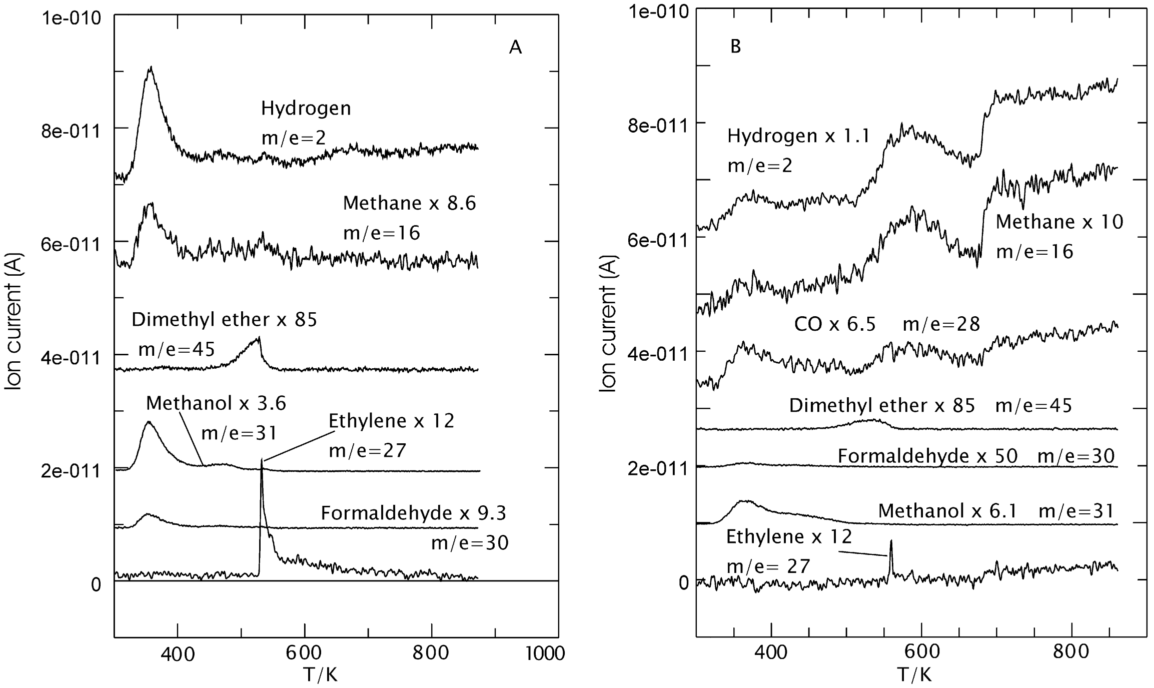

Fig. 2. TPD spectra following CH_3OH adsorption on pure ZSM-5(80) (A), 10% Mo_2C/ZSM-5(80) (B) at 300 K.

Table 1
Characteristic absorption bands following the adsorption of methanol and its decomposition products at 300 K

Mode	Gas phase CH_3OH	CH_3OH Pd/SiO_2 [44]	CH_3OH $Mo_2C/Mo(100)$ [47]	CH_3OH ZSM-5 Present study	CH_3OH Mo_2C/ZSM-5 Present study	CH_3–O–CH_3 ZSM-5 Present study	C_2H_4 Mo_2C/ZSM-5 Present study
γ_{OH}	3681						
$\nu_{as}CH_3$	3000	2956	2936	(2993) 2958	(2996) 2958	2972	2920
$\nu_{as}(CH_2)$						2947	
ν_sCH_3	2844	2846		2857	2856	2842	2852
ν_aCH_2			1441				
$\delta_{as}CH_3$	1477	1474		1468	1472, 1465	1457	1477
δ_sCH_3	1455	1454	1150	1405	1404	1427	1441
γ_aCH_3							1379
CH_2-wag (s)							
νCC			1021				
νCO	1033						

Table 2
Characteristic data for the reaction of methanol on various catalysts[a]

Catalyst	Temperature (K)	Selectivity (%)									
		CO	Methane	Ethylene	Ethane	Propylene	Benzene	Toluene	Xylenes	C_{9+}	$\sum$aromatics
ZSM-5(30)	773	0.6	6.3	15.5	2.4	12.5	2.6	8.2	12.7	6.7	30.2
	823	1.2	13.3	17.7	2.0	11.1	3.0	9.4	14.7	9.4	36.5
2% Mo_2C/ZSM-5(30)	773	0.7	7.7	13.7	1.8	10.9	3.6	10.1	14.5	8.7	36.9
	823	2.6	19.0	13.8	1.6	7.2	5.6	13.4	16.6	9.2	44.8
5% Mo_2C/ZSM-5(30)	773	5.0	28.3	9.9	1.5	3.1	3.6	12.2	17.4	13.4	46.2
10% Mo_2C/ZSM-5(30)	773	17.8	47.0	8.2	2.2	1.7	1.6	4.6	4.9	5.0	16.0
ZSM-5(80)	773	0.0	2.4	19.8	0.9	24.1	1.6	5.6	9.3	3.7	20.3
	823	0.6	7.9	18.9	1.2	20.4	2.1	7.2	12.9	6.2	28.3
2% Mo_2C/ZSM-5(80)	773	0.4	4.9	16.4	0.7	21.4	0.4	6.9	12.4	5.4	25.1
	823	2.1	17.0	13.9	0.9	12.1	0.2	8.9	17.7	12.3	39.0
5% Mo_2C/ZSM-5(80)	773	1.9	19.7	6.8	1.0	3.8	2.5	9.0	22.3	29.1	62.8
	823	6.6	32.6	5.9	1.1	1.7	2.2	6.4	12.1	28.3	49.1
10% Mo_2C/ZSM-5(80)	773	6.0	35.0	9.7	1.5	3.6	2.3	8.2	16.9	11.2	38.6
	823	2.2	21.4	12.0	1.0	9.0	1.7	7.0	19.7	14.9	43.2
ZSM-5(280)	773	0.0	0.9	18.6	0.2	44.6	0.3	2.6	3.3	0.8	7.0
	823	0.0	1.7	22.3	0.3	45.9	0.1	3.1	3.2	0.6	7.0
2% Mo_2C/ZSM-5(280)	773	0.0	2.1	16.0	0.3	41.0	0.3	4.3	5.8	1.8	12.2
	823	0.6	5.4	20.1	0.4	39.0	0.1	6.5	6.9	1.4	15.0
5% Mo_2C/ZSM-5(280)	773	0.0	2.9	12.1	0.2	30.1	1.1	4.8	10.5	4.4	20.7
	823	1.0	9.2	17.9	0.6	28.8	3.9	10.9	12.6	2.7	30.0
10% Mo_2C/ZSM-5(280)	773	0.7	4.7	15.3	0.4	28.3	2.0	9.6	11.0	3.2	25.8
	823	2.7	17.8	16.2	0.9	19.2	3.5	11.4	14.7	4.8	34.4

[a] The conversion of methanol at 773–823 K was ∼100%. Data were taken at 75 min of the reaction.

ually increased and that for butene decreased with increasing temperature. The selectivities of aromatics, toluene, xylene, and benzene, were affected only slightly by the changing temperature. Interestingly, methane, which was the main hydrocarbon product on Mo_2C/SiO_2 catalysts, was formed only above 773 K with low selectivity. The effect of temperature on the production of several compounds on ZSM-5(80) is shown in Fig. 3A. Note that the conversion and the product distribution on this sample remained the same even after 10 h of reaction at 773 K.

Depositing Mo_2C on ZSM-5 slightly enhanced the conversion at low temperature and appreciably influenced the product distribution and its temperature dependence. This is illustrated for 5% Mo_2C/ZSM-5(80) in Fig. 3B. Whereas the selectivity of ethylene varied between 5 and 8% in the temperature range of 573–873 K, that for propylene increased from 3.5% at 573 K to 15% at 723 K, then fell to ∼7% at 773 K. The selectivity of methane was very low, 1.5–3%, at 573–673 K, but increased dramatically at high temperature, to 20% at 773 K. On this sample, the selectivity of aromatics grew gradually with increasing temperature, with the highest value obtained at 773 K. Following the reaction in time on stream at 773 K, we experienced an ini-

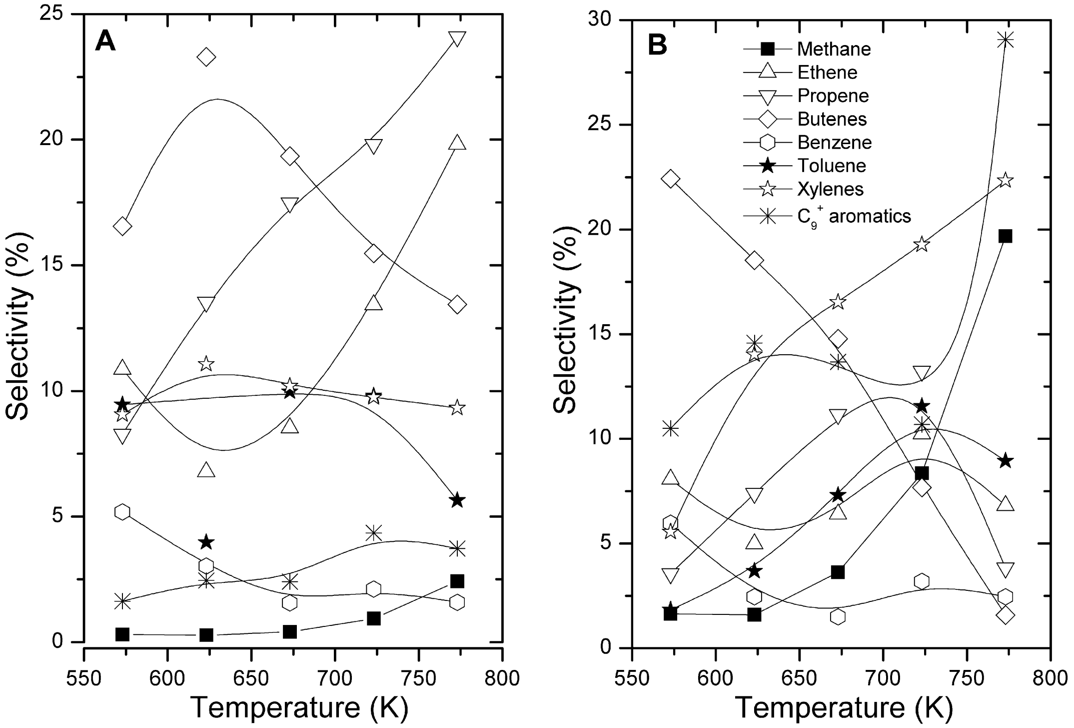

Fig. 3. Reaction of methanol over ZSM-5(80) (A) and 5% Mo_2C/ZSM-5(80) (B) at different temperatures. Data were obtained during gradual heating. At every temperature the sample was kept for 75 min.

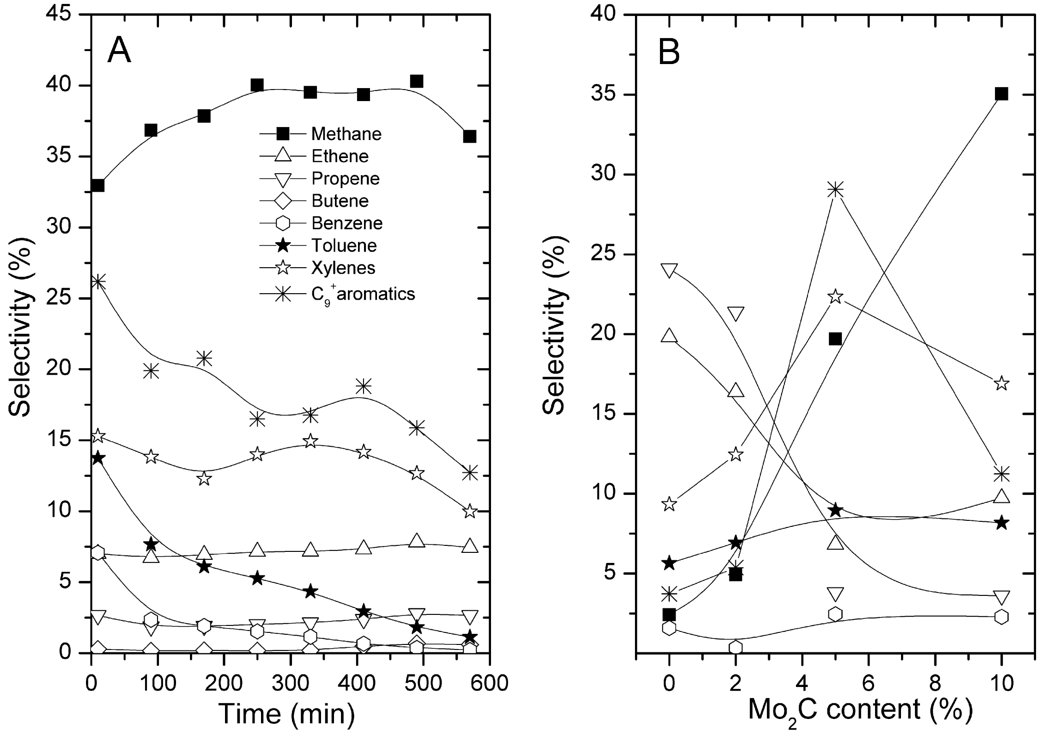

Fig. 4. Changes in the selectivity of various products on 5% Mo_2C/ZSM-5(80) at 773 K in time on stream (A). Effects of Mo_2C content of ZSM-5(80) on the selectivities of various products formed at 773 K (B). Data were taken at 75 min of the reaction.

tial decline in the selectivity of toluene and C_{9+} aromatics (Fig. 4A).

The effect of Mo_2C content on the representative data is shown in Fig. 4B. In terms of aromatization, a more marked promoting effect was experienced using 5% Mo_2C. At the optimum temperature (773 K), the selectivity of total aromatics reached 63%, twice than that found on Mo_2C-free ZSM-5(80) (Table 2). This is due mainly to the dramatically enhanced formation of C_{9+} aromatics. Further increases in Mo_2C content produced somewhat less selective catalysts.

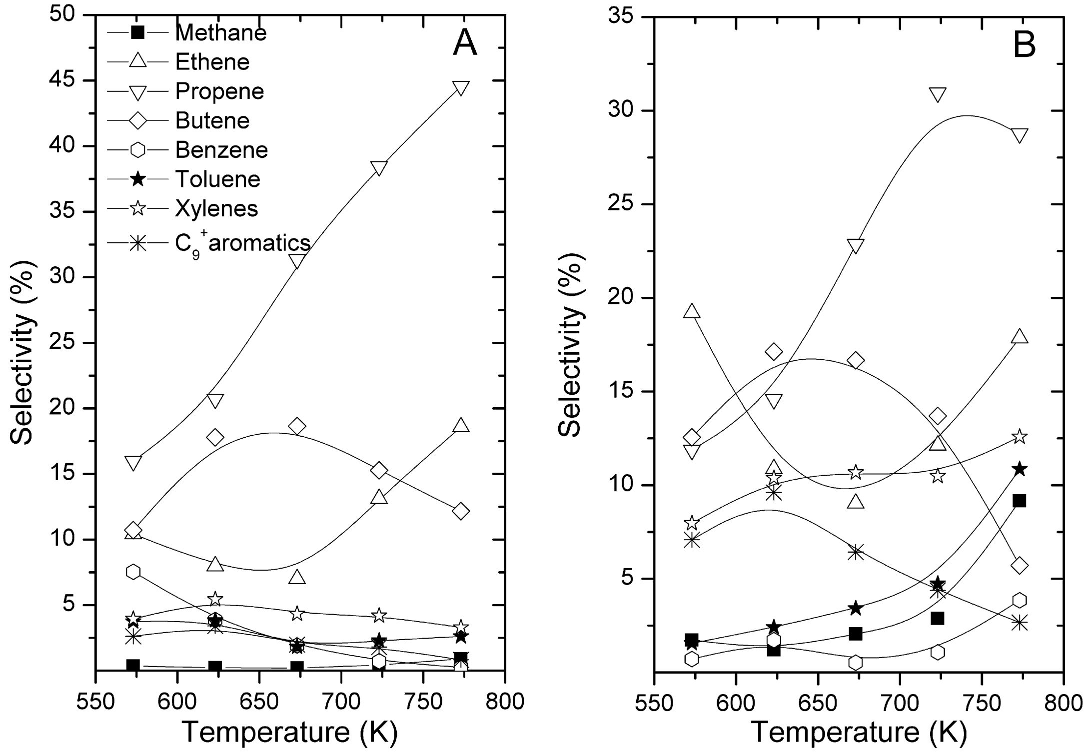

Fig. 5. Reaction of methanol over ZSM-5(280) (A) and 5% Mo_2C/ZSM-5(280) (B) at different temperatures. Data were obtained during gradual heating. At every temperature the sample was kept for 75 min.

The temperature dependence of the reaction for the ZSM-5(280) sample is presented in Fig. 5A. Adding Mo_2C to this ZSM-5 also enhanced its performance in terms of the formation of aromatics (Fig. 5B). The highest selectivity value (30%) for the total aromatics on 5% Mo_2C/ZSM-5(280) was attained at 823 K. Important data for the reaction of methanol on ZSM-5 (280)-based catalysts are also collected in Table 2. Note that repeating the measurements on Mo_2C-containing samples, we found some scattering in selectivity, but the general features of catalytic performance remained the same.

Next, we examined the effect of space velocity on the formation of various compounds. Previous studies have shown that the product distribution sensitively depends on the contact time of the methanol [9,11,12]. To decrease the conversion, we used only 0.1 g of catalyst. The conversion of methanol and the selectivity of aromatics and olefins decreased with increasing flow rate on both the pure and Mo_2C-containing ZSM-5(80). This tendency was compensated for by the increased selectivity of dimethyl ether, which was hardly detectable at low space velocity. Whereas on pure ZSM-5(80), this change was not extensive, on 5% Mo_2C/ZSM-5, all of the CH_x products disappeared at higher space velocities, and only dimethyl ether was formed. The results obtained for pure and 5% Mo_2C/ZSM-5(80) are displayed in Fig. 6B.

3.3.3. TPR measurements for used catalyst

The amount and the reactivity of coke deposited on the catalysts during the reaction was determined based on its TPR with hydrogen. The samples were treated with the reacting gas mixture for 12 h at 773 K, then cooled to room temperature in argon flow. Some TPR curves are displayed in Fig. 7. The hydrogenation of carbon started at ∼700 K yielding methane ($T_p = 873$ K) and small amounts of ethylene ($T_p = 848$ K), ethane, and propylene ($T_p = 823$ K). The total amount of carbon was 0.36 mg_C/g_{cat}. The peak temperatures agree well with those determined after the reaction of several hydrocarbons on Mo_2C/ZSM-5(80) prepared in the same manner [22–24]; however, much less coke was formed in the aromatization of methanol.

3.4. Study of the reaction between methanol and benzene

It has been reported previously that the methylation of benzene to C_7–C_{9+} aromatics can be easily realized by methanol over acidic ZSM-5 catalysts at 673 K [13–16]. Because these aromatic compounds are formed with increased selectivities and yields on Mo_2C-doped ZSM-5, it appears likely that they are produced in secondary processes also promoted by Mo_2C. As shown in Fig. 8, flowing benzene + methanol gas mixture through Mo_2C/ZSM-5 catalyst at 573–773 K, a significant enhancement in the rate of formation of C_7–C_{9+} aromatics occurred compared with the case in which benzene was not present. Note that benzene underwent very little decomposition in this temperature range, so its products make a negligible contribution to the methylation of benzene. Repeating this experiment with Mo_2C-free zeolite, we also found enhanced formation of methylated benzene, but with much lower yields than on the Mo_2C/ZSM-5 catalyst under the same experimental conditions.

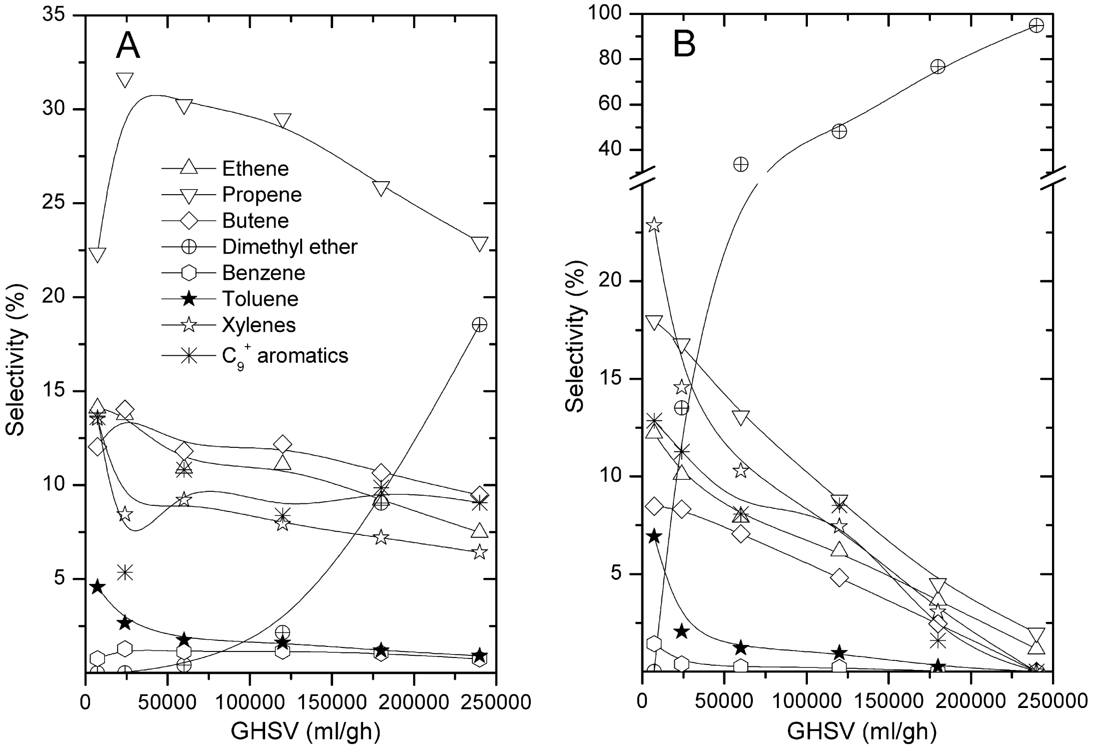

Fig. 6. Effects of space velocity on the product selectivity over ZSM-5(80) (A) and 5% Mo_2C/ZSM-5(80) (B) at 773 K.

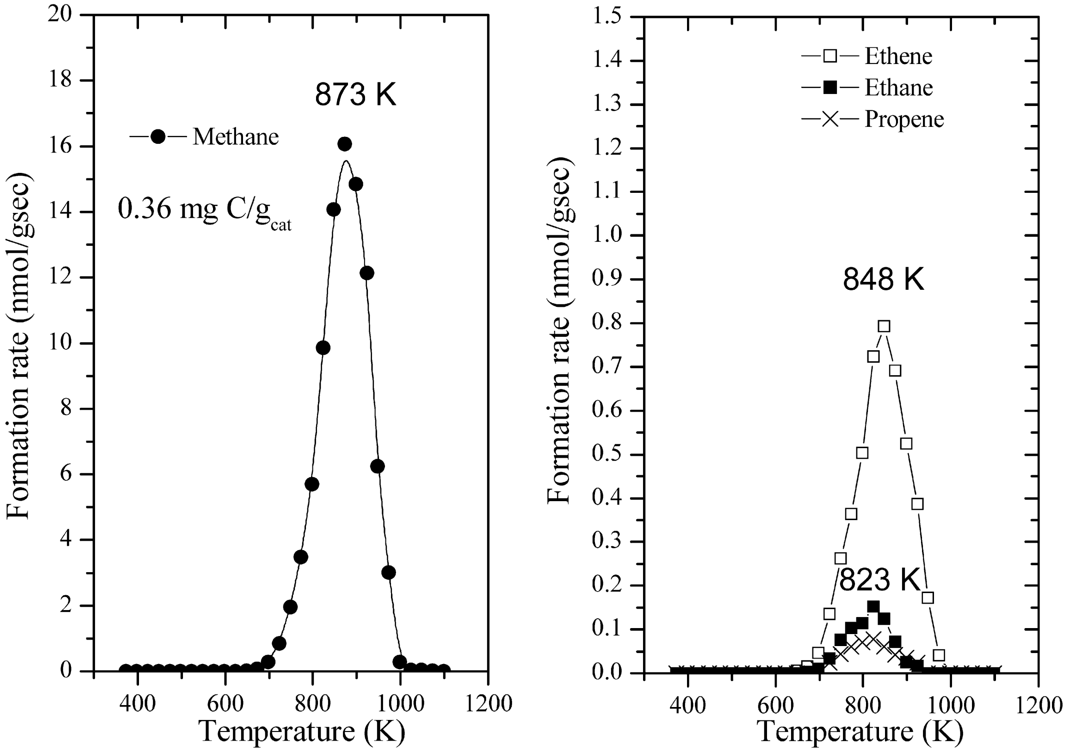

Fig. 7. Formation of hydrocarbons in the TPR measurements following methanol reaction on 5% Mo_2C/ZSM-5(80) at 773 K for 12 h.

4. Discussion

4.1. Adsorption and dissociation of methanol

IR spectroscopic studies showed that methanol strongly interacts with pure ZSM-5(80). The negative feature in the OH frequency range indicates that surface OH groups are consumed in the reaction with methanol. The absorption bands detected (Fig. 1 and Table 1) suggest that most of the adsorbed methanol dissociates on ZSM-5(80) at 300 K,

$$CH_3OH_{(a)} = CH_3O_{(a)} + H_{(a)} \tag{1}$$

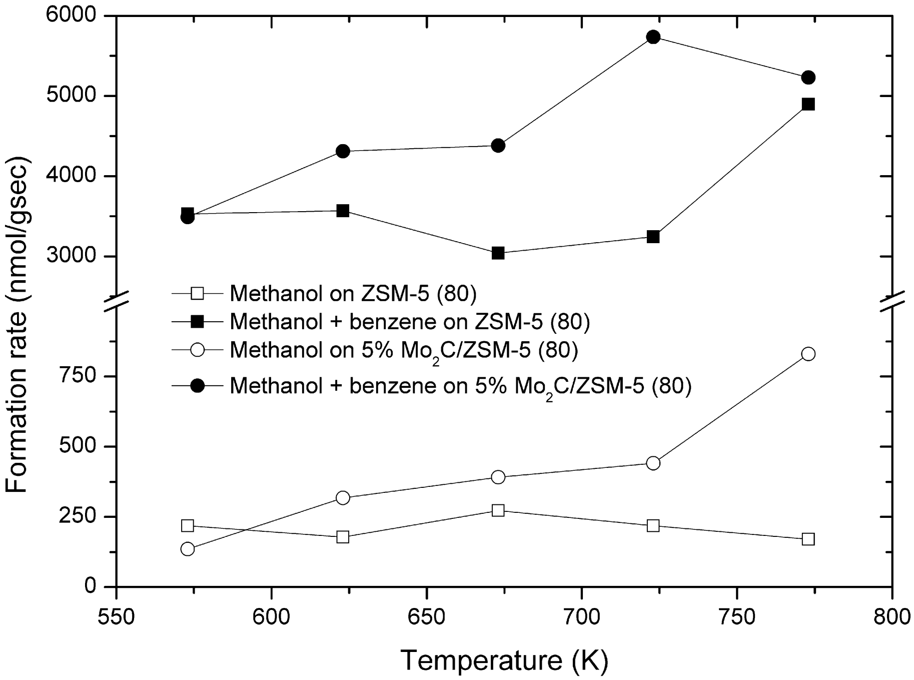

Fig. 8. Rate of formation of C_7–C_{9+} aromatics from methanol and methanol + benzene mixture (1:1) on pure ZSM-5(80) and on 5% Mo_2C/ZSM-5(80) as a function of reaction temperature. Data were obtained during gradual heating. At every temperature the sample was kept for 75 min.

and

$$H_{(a)} + OH_{(a)} = H_2O_{(g)}, \qquad (2)$$

to give methoxy species. This conclusion is supported by the positions of the $\nu_{as}(CH_3)$ and $\nu_s(CH_3)$ vibration at 2958 and 2857 cm^{-1}, respectively. Treatment of silica discs with CH_3OH in an autoclave at 300–523 K for 20 h produced methylated silicas, which gave IR bands at 2958 and 2858 cm^{-1} assigned to Si–OCH_3 compound [41]. Heating the adsorbed layer caused no significant changes in the IR spectra. Adding Mo_2C to ZSM-5 had little effect on the spectral features determined for pure ZSM-5 at 300 K (Fig. 1); the species adsorbed on ZSM-5 determine the characteristics of the spectra. After annealing the adsorbed layer at higher temperature, a weak absorption band developed at 2971 and 2925 cm^{-1}. Taking into account the characteristic spectral features of various compounds possibly formed in the reaction of adsorbed methanol (Table 1), the band at 2971 cm^{-1} can be attributed to the vibration of dimethyl ether, and the band at 2925 cm^{-1} can be ascribed to the vibration of ethylene. The formation of dimethyl ether suggests the coupling of two adsorbed methanols,

$$2CH_3OH_{(a)} = CH_3\text{–}O\text{–}CH_{3(a)} + H_2O_{(g)}. \qquad (3)$$

Careful analysis of the IR spectra of annealed layers to identify other species did not yield positive results.

TPD measurements revealed that a fraction of the adsorbed methanol on ZSM-5 desorbed and another fraction decomposed to water, hydrogen, methane, and ethylene. Very small amounts of formaldehyde and dimethyl ether also were released. We assume that the desorption of methanol is mostly the result of the associative reaction of adsorbed methoxy and hydrogen,

$$CH_3O_{(a)} + H_{(a)} = CH_3OH_{(g)}. \qquad (4)$$

The appearance of formaldehyde ($T_p = 470$ K) in the desorbing products indicates the occurrence of the dehydrogenation of methoxy species,

$$CH_3O_{(a)} = CH_2O_{(g)} + H_{(a)}. \qquad (5)$$

We expected to find CO as a result of the decomposition of formaldehyde,

$$CH_2O_{(a)} = CO_{(g)} + H_{2(g)}, \qquad (6)$$

but there was no sign of CO desorption from pure ZSM-5. We discuss the possible reaction pathway of the formation of ethylene in the following section.

The characteristics of TPD on 10% Mo_2C-containing ZSM-5 remained qualitatively the same. A new feature is the appearance of the high-temperature peaks for H_2, CO, and CH_4 (Fig. 2B), which suggests the presence of a strongly bonded C_xH_y species on the Mo_2C.

4.2. *Aromatization of methanol*

As in the case of the reaction of C_1–C_5 hydrocarbons, Mo_2C alone cannot convert methanol into aromatics; it only catalyzes its decomposition to CO, H_2, and CH_4. The situation remained the same when Mo_2C was deposited on high-surface area SiO_2. A completely different picture was found on ZSM-5-based catalysts, however. ZSM-5 alone catalyzes the conversion of methanol to olefins, and to aromatics to a lesser extent [7–16, 48–50]. Its catalytic performance depends on the Si/Al ratio or, in other words, on the number of Brönsted sites, which decreases with increasing silica content. This is reflected in the production of aromatics; the highest value was found on ZSM-5(30), and the lowest was found on ZSM-5(280) (Table 2).

Adding Mo_2C to the ZSM-5 samples significantly enhanced the formation of aromatics on all zeolite samples (Table 2). The best results were obtained at 5% Mo_2C content; any further increase in Mo_2C loading led to a decrease in the total selectivity of aromatics. This feature can be attributed to the lowering of acidic centers by Mo_2C. An exception is ZSM-5 (280), which contains fewer Brönsted sites, in which the catalytic effect of Mo_2C plays a more dominant role.

4.2.1. *Reaction of methanol on pure ZSM-5*

Before interpreting the foregoing results, it should be mentioned that because of its great technological importance, the methanol-to-olefins (MTO) process on various zeolites has been the subject of extensive research [7–16,48–50]. The central problem is the formation of C–C bonds, which is also a key step in the production of aromatics. Chang and Silvestri [8] proposed that carbene-like intermediate is produced by a concerted α-elimination mechanism involving both Brönsted-acid sites and basic sites.

Another view is that methanol is activated on the acidic sites of the catalysts to form carbenium ion, CH_3^+ [10], which reacts with methanol or dimethyl ether to give a compound containing a C–C bond,

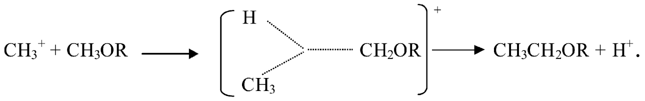

$$CH_3^+ + CH_3OR \longrightarrow \left[\begin{matrix} H \\ CH_3 \end{matrix} > \cdots CH_2OR\right]^+ \longrightarrow CH_3CH_2OR + H^+. \tag{7}$$

Several variations of these mechanisms appear in the literature. At present, most authors accept the reaction pathway, which involves the transient formation of carbenium ion. In terms of the production of aromatics, the ethylene formed should be activated, which proceeds on the Brönsted sites of ZSM-5 by the successive deprotonation of ethylene and hydride transfer to carbonium ions [4,51].

4.2.2. *Effects of Mo_2C*

When explaining the promoting effect of Mo_2C, we must take into account the fact that the deposition of Mo_2C on ZSM-5 markedly reduces the number of the acid sites of the zeolite [24]. In light of this feature, we may consider that Mo_2C opens a new route for the activation of methanol. Along with O–H bond scission proceeding on ZSM-5, cleavage of the C–O bond of adsorbed CH_3OH on Mo_2C also occurs to yield a CH_3 radical,

$$CH_3OH_{(a)} = CH_{3(a)} + OH_{(a)} \tag{8}$$

and/or

$$CH_3O_{(a)} = CH_{3(a)} + O_{(a)}, \tag{9}$$

which further decomposes to CH_2, the recombination of which leads to the formation of ethylene,

$$CH_{3(a)} = CH_{2(a)} + H_{(a)}, \tag{10}$$

$$2CH_{2(a)} = C_2H_{4(a)}. \tag{11}$$

Another fraction of CH_3 species is hydrogenated into methane,

$$CH_{3(a)} + H_{(a)} = CH_{4(g)}. \tag{12}$$

The study of the reaction pathways of CH_3 on Mo_2C/Mo (100) surface by several spectroscopic methods has disclosed that instead of its coupling into ethane, it releases hydrogen, and the recombination of CH_2 to ethylene is the favored reaction [52].

Although a huge amount of IR spectroscopic data support the cleavage of the O–H bond (i.e., the formation of methoxy species in the dissociation of methanol on solid surfaces), the rupture of the C–O bond on metals as another step is also considered. Based on XPS, SIMS, and TPD results, Winograd et al. [53] suggested a bimolecular mechanism in which two neighboring adsorbed methanol molecules produce a methoxy, a methyl group, and water on the surface. This assumption sparked an extensive debate. Yates et al. [54] found no indication of C–O bond scission by isotopic mixing studies. In harmony with this observation, we found that CH_3 produced by the photodissociation of CH_3I on Pd(100) surface is fully dehydrogenated to C around 300 K with no spectroscopic evidence for the existence of CH_2 and CH species above this temperature [55,56]. In contrast, Rebholz and Kruse [57], using field ionization spectroscopy, reported that CH_3 fragments formed at 200 K are stable up to 500 K. Chen et al. claimed [58] that methyl fragments are stable only up to 400 K; above this temperature, they dehydrogenate to CH_2 and CH species. Recently, Morkel et al. [59] suggested that there are two competing decomposition pathways of adsorbed methanol on Pd(111): dehydrogenation to CO and H_2 and methanolic C–O bond scission. The time-dependent evolution of CO/CH_xO and of carbonaceous deposits CH_x ($x = 0$–3) was monitored; however, the existence of the latter has not been established by vibration spectroscopy.

In the light of this debate, we may count on the cleavage of the methanolic C–O bond on Mo_2C, which involves a bimolecular mechanism in which two neighboring adsorbed methanol molecules produce a methoxy and methyl species, the reaction of which leads to further products. The active sites for this step could be the carbon-deficient site on the Mo_2C surface, which may have a high affinity toward oxygen. The reactivity of this site has been exhibited in the promotion of CO dissociation at 300 K [60] and also in the scission of C–I bond in the adsorbed alkyl iodides [61]. The release of strongly bonded O in the form of CO occurred only above ~960 K [60], whereas that of adsorbed I occurred above 1050 K [61].

However, the role of the Mo_2C is not solely to open a new route for the activation of methanol to ethylene—it also catalyzes its aromatization. It is very likely that Mo_2C provides dehydrogenation centres for adsorbed ethylene resulting in different products, which are converted to aromatics on the acidic sites of ZSM-5 [62,63].

To further refine the picture, we compared the rate of aromatics formation from methanol and ethylene on Mo_2C/ZSM-5 (80) under exactly the same experimental conditions. Data presented in Fig. 9 show that the aromatization process begins at lower temperatures and occurs much more rapidly from methanol than from ethylene. This suggests that the allylic and other C_xH_y species generated in the activation of methanol have a higher tendency and reactivity for transformation into aromatics compared with the "stable" ethylene molecule. Another

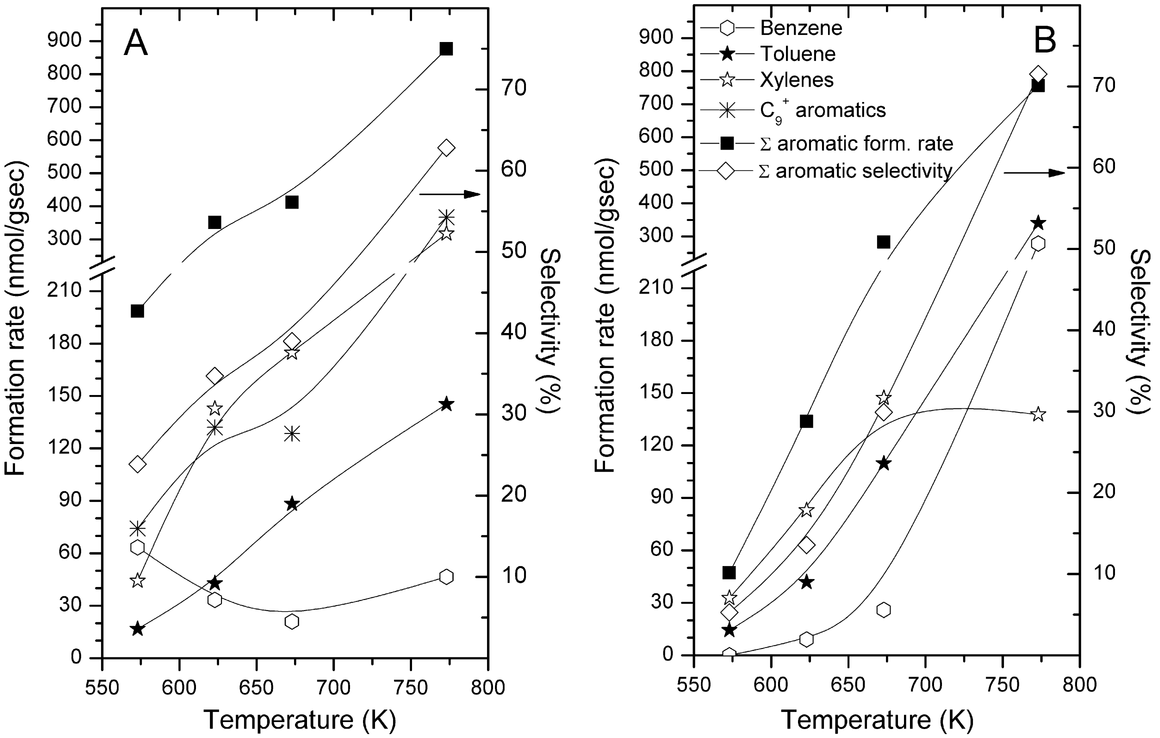

Fig. 9. Comparison of the reaction of methanol (A) and ethylene (B) on 5% Mo_2C/ZSM-5(80) at different temperatures. Data were obtained during gradual heating. At every temperature the sample was kept for 75 min. The selectivity scale refers only for total aromatics.

important feature is that greater amounts of C_8–C_{9+} aromatics are formed in the reaction of methanol compared with the reaction of ethylene. In the latter case, C_{9+} aromatics were produced only in traces. A possible reason for the different product distribution is that using methanol as a starting reagent also results in the methylation of benzene formed. This assumption has been proven by the study of the reaction between methanol and benzene. As shown in Fig. 8, the methylation of benzene with methanol occurs on pure ZSM-5; however, adding Mo_2C to the zeolite greatly promotes this process, indicating the high reactivity of hydrocarbon fragments formed in the activation of methanol.

5. Conclusions

(i) FTIR spectroscopic measurements showed that methanol adsorbs dissociatively on ZSM-5(80) at 300 K, yielding adsorbed methoxy species. This process is apparently influenced little by the presence of Mo_2C. After annealing the adsorbed layer on Mo_2C/ZSM-5, the transitory formation of dimethyl ether is also detected.

(ii) Unsupported Mo_2C is an effective catalyst for the decomposition of methanol above 573 K, yielding hydrogen, CO, CO_2, methane, and dimethyl ether. Thus is also true for silica-supported Mo_2C.

(iii) ZSM-5 zeolite also an active catalyst for the decomposition of methanol. Depending on its composition, it catalyzes the formation of aromatics at high temperatures. The deposition of Mo_2C on ZSM-5 markedly enhances the formation of aromatics (benzene, toluene, xylene, and C_{9+}), very likely by opening new routes for the activation of methanol and for the further reactions of compounds formed.

(iv) A study of the co-reaction between benzene and methanol revealed that the methylation of benzene by methanol on ZSM-5 is greatly promoted by Mo_2C, suggesting that we can count on the occurrence of this process even in the aromatization of methanol alone.

Acknowledgments

The work was supported by the Hungarian National Office of Research and Technology (NKTH) and the Agency for Research Fund Management and Research Exploitation (KPI) under contract RET-07/2005.

References

[1] D. Seddon, Catal. Today 6 (1990) 351.
[2] Y. Ono, Catal. Rev. Sci. Eng. 34 (1992) 179.
[3] M. Guisnet, N.G. Gnep, F. Alario, Appl. Catal. A Gen. 89 (1992) 1.
[4] P. Meriaudeau, C. Naccache, Catal. Rev. Sci. Eng. 39 (1997) 5, and references therein.
[5] C.D. Chang, in: G. Ertl, H. Knoezinger, J. Weitkamp (Eds.), Handbook of Heterogeneous Catalysis, VCH, Weinheim, 1997, pp. 1894–1908.
[6] G.A. Olah, Á. Molnár, Hydrocarbon Chemistry, Wiley–Interscience, New York, 2003.
[7] C.D. Chang, J.C.W. Kou, W.H. Lang, S.M. Jackob, J.J. Wise, K.J. Silvestri, Ind. Eng. Chem. Prod. Res. Dev. 171 (1978) 255.
[8] C.D. Chang, A.J. Silvestri, J. Catal. 47 (1977) 269.
[9] C.D. Chang, W.H. Lang, R.L. Smith, J. Catal. 56 (1979) 169.
[10] Y. Ono, T. Mori, J. Chem. Soc. Faraday Trans. 1 77 (1981) 2209.
[11] Y. Ono, E. Imai, T. Mori, Z. Phys. Chem. 115 (1979) 169.
[12] Y. Ono, H. Adachi, Y. Sendoda, J. Chem. Soc. Faraday Trans. 1 84 (1988) 1091.

[13] C.D. Chang, Catal. Rev. Sci. Eng. 25 (1983) 1.
[14] M.O. Adebajo, R.F. Howe, M.A. Long, Catal. Today 63 (2000) 471.
[15] M.O. Adebajo, M.A. Long, Catal. Commun. 4 (2003) 71.
[16] H.A. Zaidi, K.K. Pant, Catal. Today 96 (2004) 155.
[17] F. Solymosi, A. Szoke, Appl. Catal. 166 (1998) 225.
[18] F. Solymosi, R. Nemeth, L. Ovari, L. Egri, J. Catal. 195 (2000) 316.
[19] S. Yuan, S.B. Derouane-Abd Hamid, Y. Li, P. Ying, Q. Xin, E.G. Derouane, C. Li, J. Mol. Catal. A Chem. 184 (2002) 257.
[20] F. Solymosi, R. Nemeth, A. Szechenyi, Catal. Lett. 82 (2002) 213.
[21] F. Solymosi, A. Szechenyi, J. Catal. 223 (2004) 221.
[22] A. Széchenyi, F. Solymosi, Appl. Catal. Gen. A 306 (2006) 149.
[23] F. Solymosi, R. Barthos, Catal. Lett. 101 (2005) 235.
[24] R. Barthos, F. Solymosi, J. Catal. 235 (2005) 60.
[25] A. Széchenyi, R. Barthos, F. Solymosi, Catal. Lett. 110 (2006) 85.
[26] L. Wang, L. Tao, M. Xie, G. Xu, J. Huang, Y. Xu, Catal. Lett. 21 (1993) 35.
[27] F. Solymosi, A. Erdohelyi, A. Szoke, Catal. Lett. 32 (1995) 43.
[28] F. Solymosi, A. Szoke, J. Cserenyi, Catal. Lett. 39 (1996) 157.
[29] F. Solymosi, J. Cserenyi, A. Szoke, T. Bansagi, A. Oszkó, J. Catal. 165 (1997) 150.
[30] D.W. Wang, J.H. Lunsford, M.P. Rosynek, J. Catal. 169 (1997) 347.
[31] D. Ma, Y.Y. Shu, M.J. Cheng, X.D. Xu, X.H. Bao, J. Catal. 194 (2000) 105, and references therein.
[32] L.S. Liu, L. Wang, R. Ohnishi, M.J. Ichikawa, J. Catal. 181 (1999) 175.
[33] A.J. Brungs, A.P.E. York, J.B. Claridge, C. Marquez-Alvarez, M.L.H. Green, Catal. Lett. 70 (2000) 117.
[34] L. Leclercq, M. Provost, H. Pastor, J. Grimblot, A.M. Hardy, L. Gengembre, G. Leclercq, J. Catal. 117 (1989) 371.
[35] Á. Koós, A. Oszkó, F. Solymosi, Appl. Surf. Sci. 253 (2007) 3022.
[36] L. Ovari, F. Solymosi, J. Mol. Catal. A Chem. 207 (2004) 35.
[37] A.N. McDonald, J. Phys. Chem. 62 (1958) 175.
[38] L.D. Beliakova, A.V. Kiselev, Dokl. Akad. Nauk SSSR 119 (1958) 2.
[39] E. Borello, A. Zecchina, C. Morterra, J. Phys. Chem. 71 (1967) 2938; E. Borello, A. Zecchina, C. Morterra, J. Phys. Chem. 71 (1969) 321.
[40] C. Morterra, M.J.D. Low, J. Phys. Chem. 73 (1969) 321.
[41] N. Takezawa, H. Kobayashi, J. Catal. 25 (1972) 179.
[42] A.B. Morrow, J. Chem. Soc. Faraday Trans. 1 70 (1974) 1527.
[43] L. Kubelkova, P. Schürer, P. Jiru, Surf. Sci. 18 (1969) 245.
[44] J. Raskó, J. Bontovics, F. Solymosi, J. Catal. 146 (1994) 22.
[45] T.R. Forester, S.T. Wong, R.F. Howe, J. Chem. Soc. Chem. Commun. (1986) 1611.
[46] T.R. Forester, R.F. Howe, J. Am. Chem. Soc. 109 (1987) 5076.
[47] H.H. Hwu, J.G. Chen, Surf. Sci. 536 (2003) 75.
[48] M. Stöcker, Microporous Mesoporous Mater. 29 (1999) 3.
[49] J.F. Haw, W. Song, D.M. Marcus, J.B. Nicholas, Acc. Chem. Res. 36 (2003) 317.
[50] W. Wang, A. Bucholz, M. Seiler, M. Hunger, J. Am. Chem. Soc. 125 (2003) 15260, and references therein.
[51] M.I. Poustma, in: J.A. Rabo (Ed.), Zeolite Chemistry and Catalysis, in: ACS Monograph, vol. 171, Am. Chem. Soc., Washington, DC, 1976, p. 437.
[52] F. Solymosi, L. Bugyi, A. Oszkó, Catal. Lett. 57 (1999) 103.
[53] R.J. Levis, J. Zhicheng, N. Winograd, J. Am. Chem. Soc. 111 (1989) 4605.
[54] X. Guo, L. Hanley, J.T. Yates Jr., J. Am. Chem. Soc. 111 (1989) 3155.
[55] F. Solymosi, K. Révész, J. Am. Chem. Soc. 113 (1991) 9145.
[56] F. Solymosi, A. Berkó, Z. Tóth, Surf. Sci. 285 (1993) 197.
[57] M. Rebholz, N. Kruse, J. Chem. Phys. 95 (1991) 7745.
[58] J.-J. Chen, Z.-C. Jiang, Y. Zhou, B.R. Chakraborty, N. Winograd, Surf. Sci. 328 (1995) 248.
[59] M. Morkel, V.V. Kaichev, G. Rupprechter, H.-J. Freund, I.P. Prosvirin, V.I. Bukhtiyarov, J. Phys. Chem. B 108 (2004) 12955.
[60] F. Solymosi, L. Bugyi, A. Oszkó, Catal. Lett. 57 (1999) 103.
[61] A.P. Farkas, Á. Koós, L. Bugyi, F. Solymosi, Surf. Sci. 600 (2006) 2355.
[62] F. Solymosi, A. Szőke, Stud. Surf. Sci. Catal. 119 (1998) 355.
[63] F. Solymosi, in: E.G. Derouane, et al. (Eds.), Sustinable Strategies for the Upgrading of Natural Gas: Fundamentals, Challenges and Opportunities, Springer, New York, 2005, p. 25.